Laser Trapping of ^{225}Ra and ^{226}Ra with Repumping by Room-Temperature Blackbody Radiation

J. R. Guest,[1] N. D. Scielzo,[1] I. Ahmad,[1] K. Bailey,[1] J. P. Greene,[1] R. J. Holt,[1]
Z.-T. Lu,[1,2] T. P. O'Connor,[1] and D. H. Potterveld[1]

[1]*Physics Division, Argonne National Laboratory, Argonne, Illinois 60439, USA*
[2]*Department of Physics and the Enrico Fermi Institute, University of Chicago, Chicago, Illinois 60637, USA*
(Received 15 November 2006; published 27 February 2007)

We have demonstrated Zeeman slowing and capture of neutral ^{225}Ra and ^{226}Ra atoms in a magneto-optical trap. The intercombination transition $^1S_0 \rightarrow {}^3P_1$ is the only quasicycling transition in radium and was used for laser-cooling and trapping. Repumping along the $^3D_1 \rightarrow {}^1P_1$ transition extended the lifetime of the trap from milliseconds to seconds. Room-temperature blackbody radiation was demonstrated to provide repumping from the metastable $^3P_0$ level. We measured the isotope shift and hyperfine splittings on the $^3D_1 \rightarrow {}^1P_1$ transition with the laser-cooled atoms, and set a limit on the lifetime of the $^3D_1$ level based on the measured blackbody repumping rate. Laser-cooled and trapped radium is an attractive system for studying fundamental symmetries.

PACS numbers: 32.80.Pj, 24.80.+y, 32.10.Fn, 32.80.Ys

Radium is an alkaline-earth element with no stable isotopes, and as a result has eluded detailed spectroscopic studies. Recent calculations have suggested that radium, due to its nuclear and atomic properties, is an excellent candidate for next generation fundamental symmetry tests. The observation of a permanent electric dipole moment (EDM) in an atom, molecule, or the neutron would signal the long-sought-after violation of time-reversal symmetry (T violation, or CP violation through the CPT theorem) in a composite particle. Currently, the most stringent limits on T-violating interactions in the nucleus are set by experiments that determined the atomic EDM of ^{199}Hg to be $<2.1 \times 10^{-28} e$ cm [1]. Both collective [2] and mean-field [3] calculations have predicted that radium isotopes which are characterized by nuclear octupole deformation are 2 to 3 orders of magnitude more sensitive to T-violating interactions in the nucleus than ^{199}Hg [4,5]. ^{225}Ra is a particularly promising candidate for an EDM search because it has a relatively long half-life ($t_{1/2} = 14.9$ days) and it has nuclear spin $I = \frac{1}{2}$ (like ^{199}Hg), which eliminates potential systematic electric quadrupole shifts in EDM measurements. In addition to the atomic EDM, atomic parity-violation effects are also enhanced by a few orders of magnitude in radium due to the near degeneracy between the parity-odd $^3P_1$ level and the parity-even $^3D_2$ level [6,7], which are believed to be only 5 cm^{-1} apart [8]. Conventional atomic-beam or vapor-cell approaches to these EDM or parity-violation measurements are precluded because of the scarcity and low vapor pressure of radium, respectively. Instead, a measurement on atoms laser cooled and confined in a far-off resonant optical dipole trap or lattice offers a promising path [9].

In this Letter, we report on the first realization of laser cooling and trapping of ^{225}Ra and ^{226}Ra ($t_{1/2} = 1600$ yr, $I = 0$). This is the heaviest and only the second element with no stable isotopes (after francium [10]) laser-trapped

to date. Radium is unique among alkaline-earth elements in that the weak, intercombination transition $^1S_0 \rightarrow {}^3P_1$ is the only quasicycling transition suitable for laser cooling and trapping.

The energy level structure [8] and decay rates [11] for the radium atom are shown in Fig. 1. While the strong,
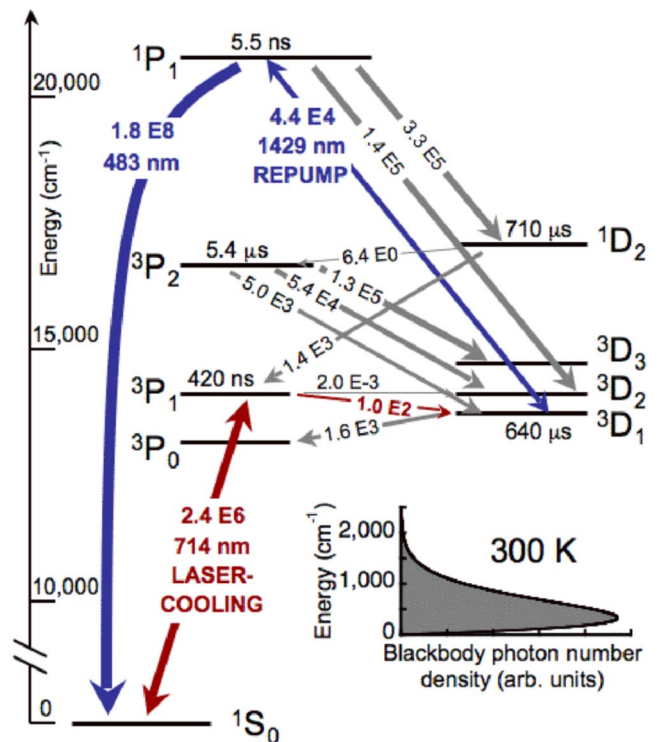

FIG. 1 (color online). Energy level diagram and decay rates for radium. Energies [8] are indicated at the left, and calculated decay rates [11] are shown ($^3P_1$ lifetime comes from experiment [12]). The 300 K blackbody photon number density is shown on the same energy scale in the inset.

singlet to singlet transition $^1S_0 \rightarrow {}^1P_1$ is exploited for efficient Zeeman slowing and first-stage cooling in Mg, Ca, Sr, and Yb, the higher-Z Ra atom is limited to ≈ 350 cycles on this transition before it decays to long-lived D levels. In contrast, the narrow intercombination $7s^2 {}^1S_0 \rightarrow 7s7p \ {}^3P_1$ transition is calculated to afford $\approx 2.4 \times 10^4$ cycles before leaking to the $7s6d \ {}^3D_1$ level [11,12]. By then repumping the atom to the $7s7p \ {}^1P_1$ level, which quickly decays back to the ground $7s^2 \ {}^1S_0$ level, we extend the number of laser-cooling transitions in the magneto-optical trap (MOT) to $\approx 3 \times 10^7$ and the laser-cooling time from tens of milliseconds to tens of seconds. As indicated by the spectrum inset in Fig. 1, room-temperature blackbody radiation can also redistribute population between the $^3P_1$, $^3D_2$, $^3D_1$, and $^3P_0$ levels.

^{226}Ra is a long-lived isotope and ^{225}Ra is an α daughter of long-lived ^{229}Th ($t_{1/2} = 7340$ yr). Typically, ≈ 0.7 μCi of ^{226}Ra (≈ 0.7 μg) and ≈ 1 mCi of ^{225}Ra (≈ 25 ng) are dissolved in 0.1 M nitric acid, pipetted onto an Al foil and placed in an oven with ≈ 50 mg of Ba metal. The Ba serves the dual purpose of reducing the $Ra(NO_3)_2$ and passivating the oven surfaces. We typically run the oven at 600–750 °C and maintain a vacuum in the trap region of $\approx 10^{-8}$ Torr.

For laser cooling along the $^1S_0 \rightarrow {}^3P_1$ transition ($\lambda = 714$ nm, $\Gamma = 2\pi \times 380$ kHz, $I_{sat} = 140$ μW/cm^2), we excite along $(J = 0) \rightarrow (J' = 1)$ for ^{226}Ra and $(F = \frac{1}{2}) \rightarrow (F' = \frac{3}{2})$ for ^{225}Ra. We use a Ti:sapphire ring laser which is referenced to molecular iodine lines. The repump $^3D_1 \rightarrow {}^1P_1$ transition is excited with an external cavity diode laser at 1429 nm. The laser is locked to a Fabry-Perot cavity, which is stabilized by a He-Ne laser. For spectroscopy on the repump transition, the scanning repump laser is monitored with a wave meter and heterodyned with a second 1429 nm external cavity diode laser which is locked to the Fabry-Perot.

The atoms emitted from the oven are first laser cooled transversely in two dimensions and then slowed in a 0.9 m Zeeman slower, which can capture atoms with velocities up to 60 m/s (10^{-3} of the longitudinal velocity profile for $T \approx 700$ °C). Because our slow cycling transition and 3 cm laser beams yield a relatively low MOT capture velocity of 10 m/s, we used an integrated geometry in which the slower magnetic fields merge smoothly with the 1 G/cm MOT magnetic field. The transverse-cooling, slowing, and MOT beams are typically detuned from the atomic transition by $-3\times$, $-12\times$, and $-6\times\Gamma$ with intensities of $50\times$, $30\times$, and $20\times I_{sat}$, respectively.

After slowing and collecting atoms in the trap for ≈ 0.5 s, the transverse-cooling and slowing beams are shuttered and the MOT light is frequency shifted (typically to $-3\times\Gamma$) and attenuated (to $2\times I_{sat}$ total in all beams). By chopping the MOT light at 1 MHz (50% duty cycle) and counting the fluorescence photons while the light is off, we take advantage of the long lifetime of the $^3P_1$ to eliminate scattered laser light and gain sensitivity to single trapped
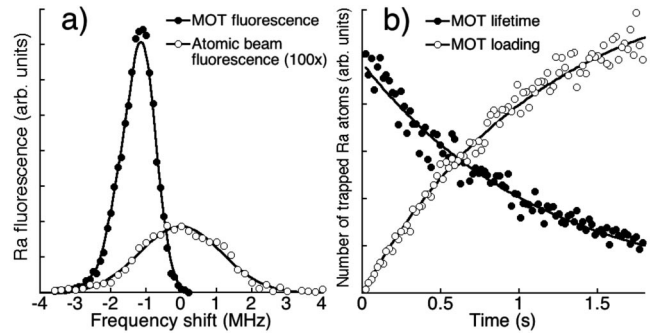

FIG. 2. Laser-trapping of ^{226}Ra atoms. (a) Spectra of the atoms in the atomic beam (multiplied by $100\times$, open circles) and laser-cooled in the MOT (solid circles). (b) The number of atoms detected in the MOT over the 1.8 s following the shuttering (unshuttering) of the slower beam at $t = 0$ yields the lifetime (loading) curve which is shown by solid (open) circles. Both curves are fit by exponentials and yield the identical lifetime $\tau = 1.1$ s for these data.

radium atoms. We can also detect the 483 nm photon from the $^1P_1 \rightarrow {}^1S_0$ decay to monitor the repump rate.

In Fig. 2(a), we show the fluorescence from ^{226}Ra atoms in the trap chamber as a function of MOT light frequency for both the untrapped atomic beam (multiplied by $100\times$) and the laser-cooled atoms captured in the MOT. During this probe phase, the laser is still cooling as evidenced by the asymmetric line shape and the redshift of the MOT signal with respect to the atomic-beam signal. Figure 2(b) shows exponential fits to the loading and decay curves for the radium MOT, which yield a lifetime $\tau = 1.1$ s that is consistent with the time scale for collisions with the background gas. The loading efficiency of the MOT can be defined as $\epsilon = L/F = N/(F\tau)$, where L is the loading rate, F is the atomic flux from the oven, and N is the number of atoms observed in the trap. The atomic flux F of ^{225}Ra is obtained by exposing a deposition target to the atomic beam and subsequently counting *in situ* the number of 40 keV gamma rays emitted during the radioactive decay of the ^{225}Ra nuclei using a germanium detector; the ^{226}Ra flux is estimated by scaling from the ^{225}Ra flux by the quantities introduced into the oven. Typically, we observe fluxes of 3×10^7 s^{-1} and 10^9 s^{-1} and atom trap numbers of 20 and 700 for ^{225}Ra and ^{226}Ra, respectively, yielding approximate efficiencies of $\epsilon \approx 7 \times 10^{-7}$ for both isotopes.

Absolute frequencies of the laser-cooling $^1S_0 \rightarrow {}^3P_1$ transitions can be extracted based on the known iodine line positions [13,14]. The energies for ^{225}Ra and ^{226}Ra are 13 999.269(1) cm^{-1} [12] and 13 999.357(1) cm^{-1}, respectively. The value for ^{226}Ra differs by 700 MHz from Moore's value [8] of 13 999.38 cm^{-1} which is based on the 1934 measurements by Rasmussen [15].

As shown in the inset of Fig. 1, thermal blackbody radiation at 300 K should be expected to play an important role in redistributing population between the $^3P_1$, $^3D_2$, $^3D_1$, and $^3P_0$ levels. Recognizing that our cold atoms are

sitting in a bath of room-temperature thermal photons, we can follow Einstein's simple treatment to relate the spontaneous emission rates A_{ji} to the thermal transition rates $\tilde{B}_{ij}(T) = B_{ij}\rho(\omega_{ij}, T)$, where $\rho(\omega_{ij}, T)$ is the blackbody photon energy density and B_{ij} is the Einstein B coefficient. For the levels in the inset of Fig. 3, we have

$$\tilde{B}_{ij}(T) = \frac{g_j}{g_i} \frac{A_{ji}}{e^{(E_j - E_i)/k_B T} - 1}, \tag{1}$$

where g_i is the degeneracy of the ith level, E_i is the energy of the ith level, and k_B is the Boltzmann constant. Taking the theoretical value for the decay along $^3D_1 \rightarrow {}^3P_0$ of $A_{21} = 1.6 \times 10^3 \text{ s}^{-1}$ [11] and the measured energy difference of 638 cm^{-1} [8], we calculate a thermal transition rate from $^3P_0 \rightarrow {}^3D_1$ of $\tilde{B}_{12} = 2.2 \times 10^2 \text{ s}^{-1}$ for our chamber temperature of $T = 296(3)$ K. Therefore, room-temperature blackbody radiation can drive population between these levels on millisecond time scales, as indicated by the curved arrows in the inset of Fig. 3.

This blackbody radiation mechanism can be seen directly in the data shown in Fig. 3, where we show the observed rate of repumping when shuttering and unshuttering the 1429 nm repump laser (solid circles) while the MOT light (714 nm) is left on. This repumping rate is measured directly as a function of time by recording the number of repump-induced 483 nm photons detected from the decay of the $^1P_1$ level (as shown in Fig. 1). When the repump laser is shuttered for the first 5 ms, population that leaks during laser-cooling accumulates in the $^3D_1$ level and, after radiative decay, in the metastable $^3P_0$ level. When the repump laser is reapplied to the cold atoms at $t = 5$ ms, the atoms residing in the $^3D_1$ level are quickly repumped and produce the short burst of 483 nm photons seen in Fig. 3. The slowly decaying exponential tail following this initial pulse corresponds to the emptying of the metastable $^3P_0$ level by thermal blackbody radiation that reexcites the atoms to the $^3D_1$ level where they can be repumped by the 1429 nm laser. The signal then settles to a steady-state repump rate.

These data are modeled effectively by a double exponential plus an offset for $t > 5$ ms, shown by the solid line in Fig. 3. The time scale for the first exponential corresponds to the laser repump rate and the time scale for the second exponential corresponds to the blackbody repump rate. This fit yields a blackbody repump rate of $\tilde{B}_{12} = 2.8 \times 10^2 \text{ s}^{-1}$, which, through Eq. (1), yields a lifetime for the $^3D_1$ level of $510 \pm 60 \ \mu$s for our chamber temperature. We interpret this as a lower limit on the lifetime because other loss mechanisms from the $^3P_0$ level could contribute to the decay of this curve.

In practice, this blackbody mechanism eases the requirements on the repumping laser fields because atoms which decay from the $^3D_1$ level to the metastable $^3P_0$ level will be recycled to the $^3D_1$ level by the thermal radiation and be exposed to the repumping laser again. This is particularly significant for ^{225}Ra, which can be efficiently repumped by
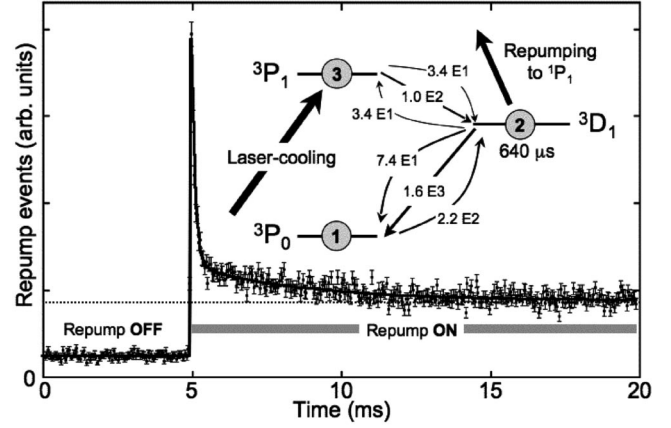

FIG. 3. Repump events (483 nm photons) observed versus time as the repump laser is shuttered and unshuttered (laser-cooling is on continuously). Experimental data (solid circles) and a double exponential fit (solid line for $t > 5$ ms) are shown with a dotted line indicating the steady-state repumping rate. The inset shows the relevant levels and the calculated transition rates due to spontaneous emission (straight arrows) and thermal radiation (curved arrows).

exciting from only one of the hyperfine manifolds. Assuming a uniform population of the $^3P_1(F = \frac{3}{2}) \ m_F$ states in the MOT, decay to the $^3D_1(F = \frac{3}{2})$ states is favored 5:1 over decay to the $^3D_1(F = \frac{1}{2})$ states. If we repump only the $^3D_1(F = \frac{3}{2})$ states, atoms which decay to the $^3D_1(F = \frac{1}{2})$ states will further decay to the metastable $^3P_0$ level. But over the time scale of 4 ms, the atoms will be recycled due to thermal radiation (as seen in Fig. 3 for ^{226}Ra) to the $(F = \frac{3}{2})$ states and repumped. This effect can also be seen in Fig. 4, which shows the number of ^{225}Ra and ^{226}Ra atoms observed in the trap as a function of the tuning of the repump laser; the four lines for ^{225}Ra
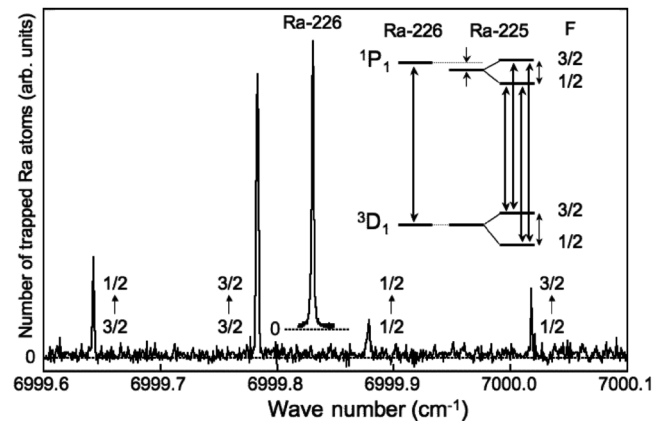

FIG. 4. Number of ^{225}Ra and ^{226}Ra atoms in the trap, as measured by fluorescence at 714 nm, vs. the wave number of the 1429 nm repump laser recorded by the wave meter. The ^{225}Ra data are scaled by 100× to compare to ^{226}Ra, which is offset on the vertical scale for clarity. The repump resonances are indicated in the inset level schematic.

TABLE I. Measured hyperfine structure constants A in MHz for ^{225}Ra on the repump transition compared to a previous measurement and theory (obtained by scaling calculations for ^{213}Ra [7] and ^{223}Ra [16] by the ratio of nuclear magnetic moments and the inverse ratio of the nuclear spins [17,18]).

Level	Experiment		Theory	
	This Letter	ISOLDE [18]	[7]	[16]
$^3D_1$	4687.7 (1.5)		4915	4981
$^1P_1$	2797.3 (1.5)	2796.5 (2.5)	1972	2688

correspond to $(F = \frac{1}{2}, \frac{3}{2}) \rightarrow (F' = \frac{1}{2}, \frac{3}{2})$ as indicated in the inset. While most efficient along $(F = \frac{3}{2}) \rightarrow (F' = \frac{3}{2})$, repumping on any of the four transitions leads to a significant increase $(10 \times -100 \times)$ in the number of trapped ^{225}Ra atoms.

By comparing the center frequencies of the ^{225}Ra and ^{226}Ra lines, we have measured the isotope shift on the $^3D_1 \rightarrow {}^1P_1$ transition to be $\nu^{226} - \nu^{225} = 540.2(2.0)$ MHz. We have also extracted the hyperfine structure constants A for ^{225}Ra, where the hyperfine energy splitting $E(F = \frac{3}{2}) - E(F = \frac{1}{2}) = \frac{3}{2} hA$. These values are presented in Table I and compared with theory [7,16]. Our measurement agrees well with the previous measurement of A for the $^1P_1$ state at ISOLDE [18].

Figure 4 also shows that the $^3D_1 \rightarrow {}^1P_1$ repump transition energy in ^{226}Ra is measured to be 6999.84(2) cm^{-1}. This confirms Russell's 1934 adjustment [19] to the original arc spectrum published by Rasmussen [15], which shifted the D-level and F-level energies by $+628$ cm^{-1}. This measurement resolves the conflict between calculations which were consistent with the correction [11,20] and theoretical concerns that these levels could be much lower in energy [21], which would have presented much stronger leak channels from the $^3P_1$ level and therefore made laser-cooling significantly more difficult. It also suggests that the apparent near degeneracy of the $^3P_1$ and $^3D_2$ levels [8] which would enhance atomic parity-violation effects in radium should be correct [6,7].

The successful laser trapping of ^{225}Ra and ^{226}Ra has opened the possibility of studying fundamental symmetries with cold, trapped radium atoms. Furthermore, to our knowledge, this is the first demonstration that blackbody radiation can serve as an effective repump source. This mechanism may find more uses in laser-trapping of atoms with complex structure [22]. In an EDM search, we estimate that a statistical sensitivity of $10^{-26} e$ cm can be achieved using a 10 mCi ^{225}Ra source with the demonstrated trapping efficiency. Because of radium's enhanced sensitivity to nuclear T-violating interactions, a search

with this level of sensitivity would be competitive with the best current limits set in the nuclear sector [1].

[1] M. V. Romalis *et al.*, Phys. Rev. Lett. **86**, 2505 (2001).
[2] N. Auerbach, V. V. Flambaum, and V. Spevak, Phys. Rev. Lett. **76**, 4316 (1996); V. Spevak, N. Auerbach, and V. V. Flambaum, Phys. Rev. C **56**, 1357 (1997); V. V. Flambaum and V. G. Zelevinsky, *ibid.* **68**, 035502 (2003).
[3] J. Engel, J. L. Friar, and A. C. Hayes, Phys. Rev. C **61**, 035502 (2000); J. Engel *et al.*, *ibid.* **68**, 025501 (2003); J. Dobaczewski and J. Engel, Phys. Rev. Lett. **94**, 232502 (2005).
[4] V. A. Dzuba *et al.*, Phys. Rev. A **66**, 012111 (2002).
[5] J. H. de Jesus and J. Engel, Phys. Rev. C **72**, 045503 (2005).
[6] V. V. Flambaum, Phys. Rev. A **60**, R2611 (1999).
[7] V. A. Dzuba, V. V. Flambaum, and J. S. M. Ginges, Phys. Rev. A **61**, 062509 (2000).
[8] C. E. Moore, Atomic Energy Levels, Vol. III, Natl. Stand. Ref. Data Ser., Nat. Bur. Stand. (U.S.), No. 35 (1971); reprint of Natl. Bur. Stand. (U.S.) Circ. 467 (1958).
[9] M. V. Romalis and E. N. Fortson, Phys. Rev. A **59**, 4547 (1999); C. Chin *et al.*, *ibid.* **63**, 033401 (2001).
[10] J. M. Simsarian *et al.*, Phys. Rev. Lett. **76**, 3522 (1996); Z.-T. Lu *et al.*, *ibid.* **79**, 994 (1997).
[11] V. A. Dzuba and J. S. M. Ginges, Phys. Rev. A **73**, 032503 (2006); V. A. Dzuba and V. V. Flambaum, J. Phys. B **40**, 227 (2007).
[12] N. D. Scielzo *et al.*, Phys. Rev. A **73**, 010501(R) (2006).
[13] S. Gerstenkorn, J. Verges, and J. Chevillard, *Atlas du Spectre D'Absorption de la Molecule D'Iode* (Laboratoire Aime Cotton, Orsay, France, 1982).
[14] H. Knöckel, B. Bodermann, and E. Tiemann, Eur. Phys. J. D **28**, 199 (2004).
[15] E. Rasmussen, Z. Phys. **87**, 607 (1934).
[16] J. Bieroń and P. Pyykkö, Phys. Rev. A **71**, 032502 (2005); J. Bieroń, J. Phys. B **38**, 2221 (2005).
[17] E. Arnold *et al.*, Phys. Rev. Lett. **59**, 771 (1987).
[18] S. A. Ahmad *et al.*, Phys. Lett. B **133**, 47 (1983); K. Wendt *et al.*, Z. Phys. D **4**, 227 (1987).
[19] H. N. Russell, Phys. Rev. **46**, 989 (1934).
[20] E. Eliav, U. Kaldor, and Y. Ishikawa, Phys. Rev. A **53**, 3050 (1996).
[21] J. Bieroń *et al.*, J. Phys. B **37**, L305 (2004).
[22] J. J. McClelland and J. L. Hanssen, Phys. Rev. Lett. **96**, 143005 (2006).